

# Self-phase-modulation-based 2R regenerator including pulse compression and offset filtering for 42.6 Gbit/s RZ-33% transmission systems

Thanh Nam Nguyen,<sup>1,\*</sup> Thierry Chartier,<sup>1</sup> Laurent Bramerie,<sup>1</sup> Mathilde Gay,<sup>1</sup> Quang Trung Le,<sup>1</sup> Sebastien Lobo,<sup>1</sup> Michel Joindot,<sup>1</sup> Jean-Claude Simon,<sup>1</sup> Julien Fatome,<sup>2</sup> and Christophe Finot<sup>2</sup>

<sup>1</sup>Laboratoire Foton, UMR 6082 CNRS-Université de Rennes 1, Ecole Nationale Supérieure des Sciences Appliquées et de Technologie, 6 rue de Kerampon, 22300, Lannion, France.

<sup>2</sup>Institut Carnot de Bourgogne, UMR 5209 CNRS-Université de Bourgogne, 9 Av. Alain Savary, BP 47870, 21078 Dijon, France.

\*Thanh-Nam.Nguyen@enssat.fr

**Abstract:** We report on the experimental and theoretical study of a self-phase-modulation-based regenerator at 42.6 Gbit/s with a return-to-zero 33% format. We point out some detrimental effects such as intrachannel interactions and Brillouin scattering. An efficient solution, relying on a self-phase-modulation-based pulse compressor in combination with the regenerator, is proposed to overcome these detrimental phenomena. The experimental demonstration shows the effectiveness of a wavelength-transparent regenerator at 42.6 Gbit/s with a sensitivity-improvement of more than 5 dB and an eye-opening improvement of 2.3 dB in a back-to-back configuration, as well as a 10 times maximum transmission distance improvement for a BER of  $10^{-4}$ .

©2009 Optical Society of America

**OCIS codes:** (060.2330) Fiber optics communications; (190.3270) Kerr effect; (190.4380) Nonlinear optics, four-wave mixing; (070.4340) Nonlinear optical signal processing.

---

## References and links

1. G. P. Agrawal, *Fiber-Optic Communication Systems* (Wiley-Interscience, 2002).
2. P. V. Mamyshev, "All-optical data regeneration based on self-phase modulation effect," in Proceedings of European Conference on Optical Communication (Institute of Electrical and Electronics Engineering, Madrid, Spain, 1998), pp. 475–476.
3. G. Raybon, Y. Su, J. Leuthold, and R. J. Essiambre, T.-H.-. Her, C. Joergensen, P. I. Steinvurze, K. Dreyer, and K. S. Feder, "40 Gbits/s pseudo-linear transmission over one million kilometers," in Proceedings of Optical Fiber Communication Conference (Anaheim, USA, 2002), Paper PD FD 10, pp 1–3.
4. T.-H. Her, G. Raybon, and C. Headley, "Optimization of pulse regeneration at 40 Gb/s based on spectral filtering of self-phase modulation in fiber," *IEEE Photon. Technol. Lett.* **16**(1), 200–202 (2004).
5. M. Matsumoto, "Efficient all-optical 2R regeneration using self-phase modulation in bidirectional fiber configuration," *Opt. Express* **14**(23), 11018–11023 (2006), <http://www.opticsinfobase.org/oe/abstract.cfm?URI=oe-14-23-11018>.
6. M. Matsumoto, Y. Shimada, and H. Sakaguchi, "Two-stage SPM-based all-optical 2R regeneration by directional use of a highly nonlinear fiber," *IEEE J. Quantum Electron.* **45**(1), 51–58 (2009).
7. M. Rochette, L. B. Fu, V. G. Ta'eed, D. J. Moss, and B. J. Eggleton, "2R optical regeneration: an all-optical solution for BER improvement," *IEEE J. Sel. Top. Quantum Electron.* **12**(4), 736–744 (2006).
8. B. E. Olsson, and D. J. Blumenthal, "Pulse restoration by filtering of self-phase modulation broadened optical spectrum," *J. Lightwave Technol.* **20**(7), 1113–1117 (2002).
9. M. Daikoku, N. Yoshikane, T. Otani, and H. Tanaka, "Optical 40-Gb/s 3R Regenerator with a combination of the SPM and XAM effects for all-optical networks," *J. Lightwave Technol.* **24**(3), 1142–1148 (2006).
10. L. Provost, F. Parmigiani, C. Finot, K. Mukasa, P. Petropoulos, and D. J. Richardson, "Analysis of a two-channel 2R all-optical regenerator based on a counter-propagating configuration," *Opt. Express* **16**(3), 2264–2275 (2008), <http://www.opticsinfobase.org/oe/abstract.cfm?URI=oe-16-3-2264>.
11. Y. Su, G. Raybon, and R. J. Essiambre, "All-optical 2R regeneration of 40 Gb/s signal impaired by intrachannel four-wave mixing," *IEEE Photon. Technol. Lett.* **15**(2), 350–352 (2003).
12. V. G. Ta'eed, M. Shokoh-Saremi, L. B. Fu, D. J. Moss, M. Rochette, I. C. M. Littler, B. J. Eggleton, Y. L. Ruan, and B. Luther-Davies, "Integrated all-optical pulse regenerator in chalcogenide waveguides," *Opt. Lett.* **30**(21), 2900–2902 (2005).

13. C. Kouloumentas, P. Vorreau, L. Provost, P. Petropoulos, W. Freude, J. Leuthold, and I. Tomkos, "All-Fiberized Dispersion-Managed Multichannel Regeneration at 43 Gb/s," *IEEE Photon. Technol. Lett.* **20**(22), 1854–1856 (2008).
14. L. A. Provost, C. Finot, P. Petropoulos, K. Mukasa, and D. J. Richardson, "Design scaling rules for 2R-optical self-phase modulation-based regenerators," *Opt. Express* **15**(8), 5100–5113 (2007), <http://www.opticsinfobase.org/oe/abstract.cfm?URI=oe-15-8-5100>.
15. C. Finot, T. Nguyen, J. Fatome, T. Chartier, S. Pitois, L. Bramerie, M. Gay, and J. Simon, "Numerical study of an optical regenerator exploiting self-phase modulation and spectral offset filtering at 40 Gbit/s," *Opt. Commun.* **281**(8), 2252–2264 (2008).
16. T. N. Nguyen, M. Gay, L. Bramerie, T. Chartier, J. C. Simon, and M. Joindot, "Noise reduction in 2R-regeneration technique utilizing self-phase modulation and filtering," *Opt. Express* **14**(5), 1737–1747 (2006), <http://www.opticsinfobase.org/oe/abstract.cfm?URI=oe-14-5-1737>.
17. T. I. Lakoba, and M. Vasilyev, "A new robust regime for a dispersion-managed multichannel 2R regenerator," *Opt. Express* **15**(16), 10061–10074 (2007), <http://www.opticsinfobase.org/oe/abstract.cfm?URI=oe-15-16-10061>.
18. T. N. Nguyen, T. Chartier, and J.-C. Simon, "Simple Rules and Chart to Design an All-optical SPM-based Regenerator," in *European Conference on Lasers and Electro-Optics (Munich, Germany, 2009)*, paper. CD.P.18.
19. G. P. Agrawal, *Nonlinear Fiber Optics*, third Ed., (San Francisco, CA: Academic Press, 2001).
20. C. Finot, B. Kibler, L. Provost, and S. Wabnitz, "Beneficial impact of wave-breaking or coherent continuum formation in normally dispersive nonlinear fibers," *J. Opt. Soc. Am. B* **25**(11), 1938–1948 (2008), <http://www.opticsinfobase.org/josab/abstract.cfm?URI=josab-25-11-1938>.
21. J. E. Rothenberg, "Colliding visible picosecond pulses in optical fibers," *Opt. Lett.* **15**(8), 443–445 (1990), <http://www.opticsinfobase.org/ol/abstract.cfm?URI=ol-15-8-443>.
22. P. V. Mamyshev, and N. A. Mamysheva, "Pulse-overlapped dispersion-managed data transmission and intrachannel four-wave mixing," *Opt. Lett.* **24**(21), 1454–1456 (1999), <http://www.opticsinfobase.org/ol/abstract.cfm?URI=ol-24-21-1454>.
23. R. J. Essiambre, B. Mikkelsen, and G. Raybon, "Intra-channel cross-phase modulation and four-wave mixing in high-speed TDM systems," *Electron. Lett.* **35**(18), 1576–1578 (1999).
24. Y. Yang, C. Lou, H. Zhou, J. Wang, and Y. Gao, "Simple pulse compression scheme based on filtering self-phase modulation-broadened spectrum and its application in an optical time-division multiplexing system," *Appl. Opt.* **45**(28), 7524–7528 (2006), <http://www.opticsinfobase.org/ao/abstract.cfm?URI=ao-45-28-7524>.
25. N. S. Bergano, F. W. Kerfoot, and C. R. Davidson, "Margin measurements in optical amplifier systems," *IEEE Photon. Technol. Lett.* **5**(3), 304–306 (1993).
26. Q. T. Le, L. Bramerie, M. Gay, G. Girault, M. Joindot, and J. C. Simon, "Noise Tolerance Assessment and System Design Discussion of a Saturable-Absorption-Based All-Optical 2R Regenerator," *IEEE Photon. Technol. Lett.* **21**(9), 590–592 (2009).

---

## 1. Introduction

With the development of long haul optical telecommunication systems working at high repetition rates (40 Gbit/s and beyond), performing all-optical 2R regeneration of the signal (Re-amplifying and Reshaping) has become of great interest to combat the cumulative impairments occurring during the signal propagation. Indeed, the signal undergoes various degradations such as noise accumulation due to amplified spontaneous emission (ASE) of optical amplifiers, chromatic dispersion as well as intra-channel nonlinear effects. These latter lead to jitter degradations (in time and amplitude) and ghost-pulse generation in the zero bit-slot [1]. Consequently, in order to improve the transmission distance, it is generally required to limit the amplitude and timing jitters of the pulses and to enhance the extinction ratio (ER) of the signal. To achieve simultaneously such operations, different optical methods based on nonlinear effects in optical fibers have been proposed. The approach based on self-phase modulation (SPM) in a fiber and offset spectral filtering, known as Mamyshev regenerator [2], is one of the most promising technique thanks to its experimental setup simplicity and its potential for high bit rate applications. Because of the intensity-dependence of spectral broadening, this system works like a nonlinear optical gate. Its power transfer function exhibits two plateaus, one for the "zero" symbols, the other one for the "one" symbols, allowing an efficient signal regeneration process. However, this technique causes also a wavelength conversion. In order for the signal wavelength to be preserved, a double-stage configuration is used to overcome this problem. It consists in a cascade of two single-stage regenerators in which the wavelength conversions cancel each other.

Since the first demonstration in 1998, many works, both experimental [3–13] and theoretical [14–18], have dealt with the Mamyshev regenerator. Despite the fact that the return-to-zero (RZ) format with duty cycles of 33% is intensively used in optical telecommunications, we have noticed that, in some experimental demonstrations of

Mamyshev regeneration [2–6], duty cycles around 25% or below are used. Such a choice of using low duty-cycle pulse trains is essentially driven by two reasons. The first one is to benefit from an expanded spectrum in order to counteract the Brillouin backscattering effect [3]. The second motivation is to avoid any intrachannel pulse-to-pulse overlapping occurring during the SPM-based spectral broadening stage. In Ref [4], for example, T.-H. Her *et al.* claimed that using duty cycles higher than 25% could involve a strong overlapping between adjacent pulses, thus stimulating the generation of undesirable spectral components. Additional numerical investigations have confirmed this last result by demonstrating a significant performance degradation of the regenerator [14,15] and pointed out the difficulty to achieve a high extinction ratio improvement without pulse level fluctuations.

In the present paper, we investigate the influence of the initial pulse duration on the performance of the single-stage Mamyshev regenerator both numerically and experimentally. Then, we propose a novel design for an efficient wavelength-transparent regenerator at 42.6 Gbit/s including a pulse compressor with an offset spectral filtering. This new configuration enables us to avoid detrimental nonlinear effects when operating with a duty cycle of 33%. Finally, the efficiency of the proposed device is carefully analyzed using a short recirculation loop setup that assesses the ability of the optical regenerator to be successfully cascaded.

## 2. Influence of the initial pulse width

### 2.1 Experimental setup

Figure 1 shows the experimental setup to study a typical Mamyshev regenerator. The emission consists of a tunable DFB laser and an external modulator at 42.6 Gbit/s generating a RZ-33% format. Note that the driven current of the DFB laser is slightly modulated. This low-frequency modulation broadens the spectrum of the signal and avoids any Brillouin effect in the fiber. The signal at 1541 nm then goes through an optical attenuator before entering the regenerator.

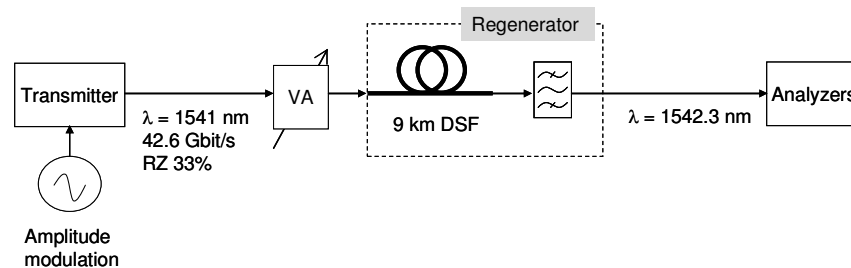


Fig. 1. Setup for the nonlinear interaction experiments. VA: variable attenuator; DSF: dispersion-shifted fiber.

The design of the regenerator is based on the simple rules proposed in Ref [14]. It consists in a 9-km long dispersion-shifted fiber (DSF) with normal dispersion  $D = -0.5$  ps/nm/km, dispersion slope  $S = 0.07$  ps/nm<sup>2</sup>/km, Kerr nonlinearity  $\gamma = 2.6$  W/km and optical loss  $\alpha = 0.25$  dB/km. The optical bandpass filter (OBPF) has a Gaussian shape with a full width at half-maximum (FWHM) of 0.41 nm. The filter is shifted by 1.3 nm with respect to the signal wavelength, corresponding to a central wavelength of 1542.3 nm. At the output of the regenerator, the signal is analyzed in terms of power, spectrum, optical waveform and eye-diagram.

The experimental transfer function of the regenerator, linking the output average power as a function of the input power, is presented in Fig. 2a and clearly exhibits the two expected plateaus required for an efficient simultaneous regeneration of the zero and one levels. The theoretical transfer function, calculated using the nonlinear Schrödinger equation (NLSE) [19], is also represented and is in excellent agreement with the experimental results.

Because of the presence of the second plateau obtained for input powers above 350 mW, we could expect an efficient equalization of the output one levels. However, the temporal

measurement of the output pulse stream using an optical sampling oscilloscope (1 ps resolution) reveals strong fluctuations in the “one” symbol levels (see the inset of Fig. 2a). The eye diagram of the output signal confirms the presence of two distinct levels for the “one” bits (Fig. 2b). In such a context, even with a well-adapted transfer function, we can conclude that the regenerator will be unable to work properly. Let us note that increasing the working power of the regenerator, as it has been suggested in [15,16], does not lead to cancel those strong level fluctuations.

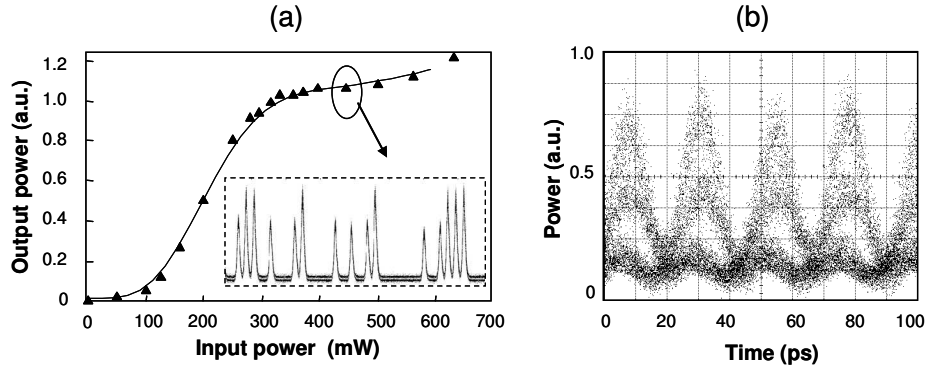


Fig. 2. (a) Experimental (triangles) and theoretical (solid line) transfer functions of the regenerator. Inset: output optical data stream for a working average power of 450 mW; (b) Eye diagram of the regenerator output signal for a working power of 450 mW.

## 2.2 Theoretical interpretation

The previous experimentally observed level fluctuations are well reproduced by numerical simulations based on the NLSE. As shown in Fig. 3, we have considered an initial pulse sequence made of the following pattern ‘10110111’ and propagating in the regenerator. Note that the parameters used in these simulations are the same as those used in our experimental setup. As can be seen in Fig. 3b, for an input average power of 450 mW, the output pulses obtained after spectral filtering exhibit a strong patterning effect undergone during the spectral broadening. It is noticeable that an isolated pulse or the first pulse of a ‘one’ sequence systematically exhibits a level below the other pulses, which is fully consistent with the experimental results of Fig. 2a. These amplitude fluctuations of the ‘one’ symbols at the output of the regenerator have also been reported by Lakoba and Vasilyev [17]. To better understand the origin of this patterning effect, we investigated the intensity and chirp profiles of the pulses obtained after propagation in the 9-km long DSF fiber and just before the offset filtering stage (Fig. 3c).

From Fig. 3c, we can point out that during its propagation in the normal dispersion fiber, a single pulse temporally broadens, undergoes a significant nonlinear reshaping and develops a nearly linear frequency chirp [20]. Consequently, when an adjacent pulse is present, the temporal broadening will lead to a non negligible pulse-to-pulse overlapping which induces a sinusoidal beating between opposite frequency chirps [21]. Due to the fiber Kerr nonlinearity, these interference patterns will then affect the phase of the pulses, and consequently the spectrum of the pulse train. As the interaction is exclusively with the nearest neighbour, this dynamic can be considered as an intrachannel cross phase modulation (IXPM) effect [22,23].

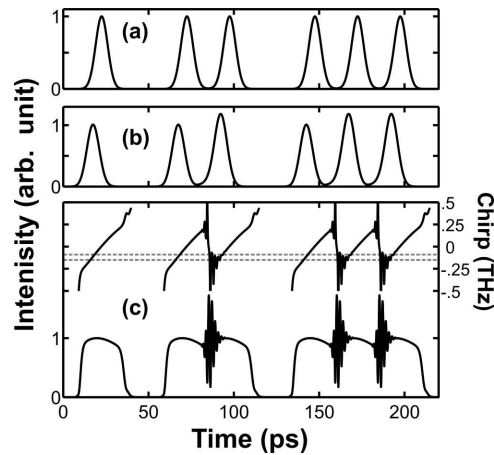


Fig. 3. Numerical simulation results. (a) Input signal; (b) Regenerator output signal for an input average power of 450 mW; (c) Intensity and chirp profiles of the pulses after propagation in the DSF fiber and before spectral filtering.

When a spectral offset filtering is now applied, it selectively isolates the lowest frequency components of the pulses, which are temporally localized in the front edge of the pulse. As it is illustrated in Fig. 3c, the leading tail of the first pulse of a sequence of “ones” is not affected by the strong oscillations, so that it is attributed to IXPM. Consequently, after filtering, we obtain the same shape as an isolated pulse. This is not the case for the other pulses of a sequence of “ones”, which explains the level fluctuations observed in Fig. 2a and Fig. 3b. Let us also add that the sign of the frequency offset of the OBPF will influence the resulting sequence. Indeed, for a positive frequency offset, the OBPF will select the frequency components localized in the trailing edge of the pulse.

Since the patterning effect is due to nonlinear interaction when pulses overlap, it might be expected that it vanishes for an appropriate choice of fiber parameters (nonlinearity, dispersion and length). However, we have observed by performing additional simulations that it still occurs with various fiber parameters for the RZ-33% format. This can be explained as follows. For a Mamyshev regenerator composed of one nonlinear fiber and one filter, it has been shown in Refs. [14,18], that the ratio between the fiber nonlinearity and the fiber dispersion, as well as the product between the fiber length and the fiber dispersion, must be equal to a given value for a given pulse duration in order to achieve a step-like transfer function. For this reason it is not possible to choose both a value of nonlinearity that ensures enough spectral broadening and a value of dispersion or length that limits the pulse overlapping. In other words, when using the RZ-33% format, the patterning effect should occur in Mamyshev regenerators based on standard fibers as well as on highly nonlinear waveguides [12].

### 2.3 Insertion of a pulse compressor

In order to reduce this detrimental overlapping phenomenon, several techniques have been proposed such as using dispersion-managed regenerators (composed of several parts of fibers) to reduce the overlapping between pulses [13,17]. Another solution, which does not need any specific design for the fiber in the regenerator, consists in using shorter pulses for the input signal [4]. Such an approach has been later confirmed by a more systematic study that outlined the benefit of the RZ-25% format compared to RZ-33% for similar working points [14].

As the RZ-33% format is largely used in the telecommunication systems, rather than changing the format of the transmitter, we have focused on limiting the intrachannel nonlinear impairments by introducing a compression stage inside the regenerator. The compression technique used in our experiment relies on a SPM-induced spectral broadening in a normally

dispersive fiber followed by a subsequent offset spectral filtering [24]. The difference between this SPM-based compressor and the Mamyshev regenerator is the value of the off centered filter bandwidth chosen in each device. A Mamyshev regenerator usually uses an off centered filter bandwidth equal to the spectral width of the signal while a SPM-based compressor uses a larger one. The minimum output pulse duration of the compressor is simply determined by the product of the SPM-induced broadened spectrum and the output spectral filter properties. The pulse compressor that we have developed is therefore based on a 7-km long DSF fiber and a tunable Gaussian-shape OBPF with a bandwidth of 0.76 nm. In such configuration, the output pulse duration can be continuously adjusted from 9 ps to 6 ps by offsetting the central wavelength of the filter.

Using this compressor, we have optimized the second stage of the regenerator with a 6 ps-pulse train. The configuration of this second stage is similar to the one depicted in Fig. 1. Let us note that changing the initial temporal pulse width also leads to a shortening of the fiber to observe the expected regeneration [14]. Therefore, the length of the DSF has been shortened from 9 km to 4 km. The filter characteristics are kept constant: 1.3-nm offset shift and 0.41-nm spectral width. The experimental transfer function is shown in Fig. 4. Besides the exhibition of two plateaus in the transfer function, we have observed that the intrachannel interaction, i.e the peak power fluctuations, are now considerably reduced (inset in Fig. 4).

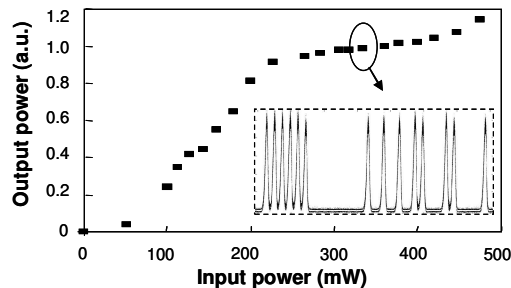


Fig. 4. Experimental transfer function of the regenerator for a 4-km long DSF and 6-ps input pulse width produced from the compressor. Inset shows the experimental data sequence at optimum power (320 mW).

It is interesting to mention that, in this experiment, the external DFB current modulation used to avoid Brillouin effect has been removed. Thanks to the 5% branch of an input coupler inserted just before the DSF, we have measured the amount of backscattering light in the 4-km long DSF fiber as a function of the input power for four different input pulse widths. Experimental results are presented in Fig. 5a and show a typical threshold-like behavior of Brillouin backscattering for different input pulse widths. In Fig. 5b, Brillouin spectral lines, red-shifted by 10 GHz with respect to the signal modulation lines, are clearly visible when 8.5-ps input pulses (RZ-33%) are launched into the regenerator at 300 mW. No Brillouin components are observed for lower pulse durations. For pulse durations below 8 ps, the spectrum is broader and the power in each modulation spectral line is below the Brillouin threshold. Note that compressing the pulses in order to suppress Brillouin scattering has already been mentioned in previous works [3,9].

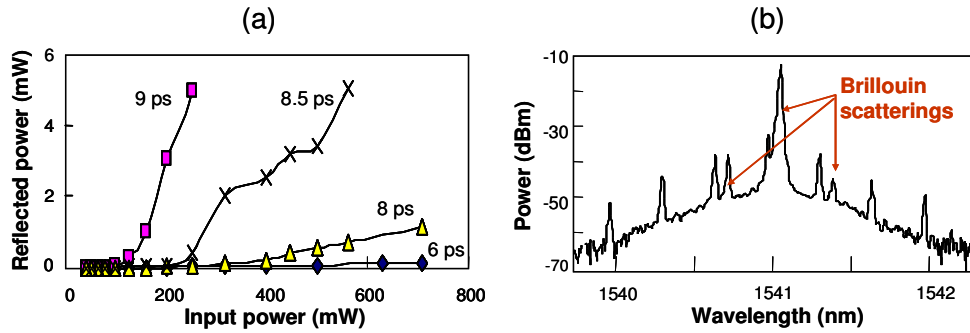


Fig. 5. (a) Evolution of the reflected power as a function of input power in the 4-km long DSF fiber for 4 different input pulse widths; (b) Spectrum of the reflected signal for a pulse width of 8.5 ps with an input power of 300 mW.

### 3. Double-stage regenerator proposition

#### 3.1 Experimental setup

Intrachannel nonlinear interactions and Brillouin scattering occurring in a nonlinear fiber for a RZ-33% pulse train are now eliminated by the association of the pulse compressor and the optimized regenerator described in the previous section. In order to fully demonstrate the potential of such a setup, we will now investigate in more details the performance of this double-stage device.

The experimental setup is described in Fig. 6. The compressor stage includes a 23 dBm erbium-doped fiber amplifier (EDFA) followed by a flat-top filter (1.2 nm spectral width) and a 7 km-long DSF fiber followed by a 0.76 nm spectral width Gaussian filter. In order to generate 6-ps pulses, we have detuned the central wavelength of the output Gaussian filter by 1 nm, so that the wavelength at the input of the regenerator stage is 1541 nm. In the second stage, the regenerator benefits from a 27 dBm EDFA associated to a flat-top filter (1.3 nm spectral width). The role of this flat-top filter in the compressor are to limit the accumulation of amplified spontaneous emission at the zone where signal will be shifted to [16]. After propagation in the 4-km long DSF fiber, the signal is finally filtered by the 0.41-nm Gaussian output filter. The filter is shifted by 1 nm so as to restore the initial wavelength of the pulse stream (1540 nm). Note that, a slight difference between the value of the wavelength shift in this regenerator (1 nm) and the value in the previous experiment (1.3 nm) does not influence much the form of the transfer function but rather reduces the working power.

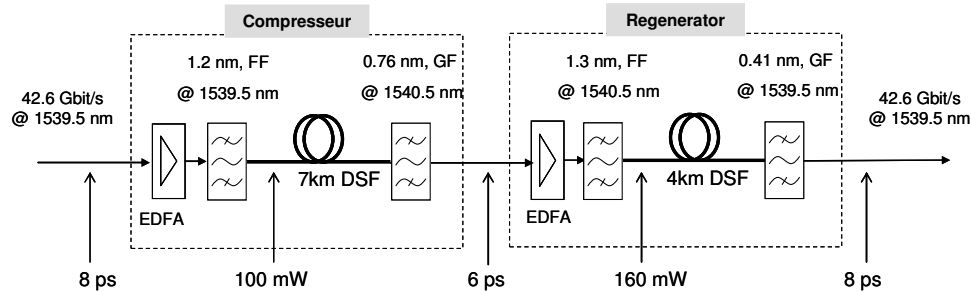


Fig. 6. Experimental setup for the proposed wavelength-transparent double-stage regenerator. FF: Flat-top filter; GF: Gaussian filter; EDFA: Erbium doped fiber amplifier; DSF: dispersion-shifted fiber.

Let us stress that our proposed configuration is different from the two-stage Mamyshev regenerators generally required to avoid wavelength conversion [5,15]. In our case, the first

stage does not perform any optical regeneration but plays the double role of pulse compression as well as wavelength conversion. This configuration is also more practical than the one proposed in Ref [3], where three devices were used, one compressor followed by a double-stage regenerator.

Moreover, the interest of our setup is not only to simplify the architecture of the device but also to reduce the power consumption. Indeed, using a compressor as a first stage does not require a step-like transfer function presenting two plateaus. The working power can then be below the power generally required to reach the second plateau. Moreover, the second stage, which plays the role of the Mamyshev regenerator, benefits from a pre-broadened spectrum from the output of the compressor. Less power is then required for the second stage to achieve the step-like transfer function presenting two plateaus. Our calculations have also shown that our configuration reduces by about 2 dB the required optical power in comparison with a conventional double-stage configuration. Note also that, thanks to less power requirement in the first stage, we did not observe any Brillouin effect during the compression process although the format of the input signal is RZ-33%.

### 3.2 Back-to-back measurements

In order to characterize the efficiency of our double stage regenerator, some measurements in a back-to-back (BTB) configuration have been performed. The setup of the BTB configuration is presented in Fig. 7. The novel double-stage regenerator (compressor + regenerator) is placed between a 42.6 Gbit/s transmitter and a receiver. A noise source, after passing a variable attenuator, is coupled to the signal. This allows determining the ability of amplitude noise reduction of the regenerator. The optical signal-to-noise-ratio (OSNR) can then be adjusted by the variable attenuator. A polarization controller (PC) is used to avoid any effect of the signal polarization.

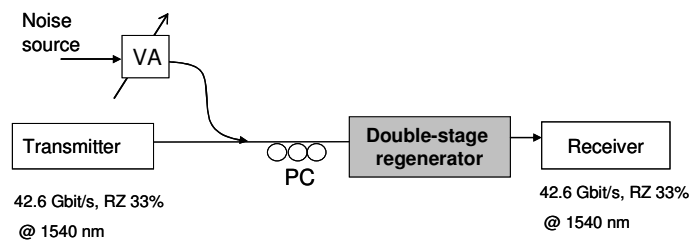


Fig. 7. Experiment setup for back-to-back characterizations. VA: variable attenuator; PC: polarization controller.

Figure 8 shows the evolution of the bit error rate (BER) as a function of the average power on the photodiode with (full symbols) and without the regenerator (empty symbols) for two different values of the OSNR (44.5 dB/1nm and 17.5 dB/1nm). With noise and without the regenerator a 5 dB penalty is observed for a BER of  $10^{-9}$  due to the excess of optical noise. When the regenerator is inserted, the curve is superimposed to the reference (no noise, no regenerator), demonstrating the good ability of the device to reduce noise and confirming that our regenerator does not introduce any power penalty.

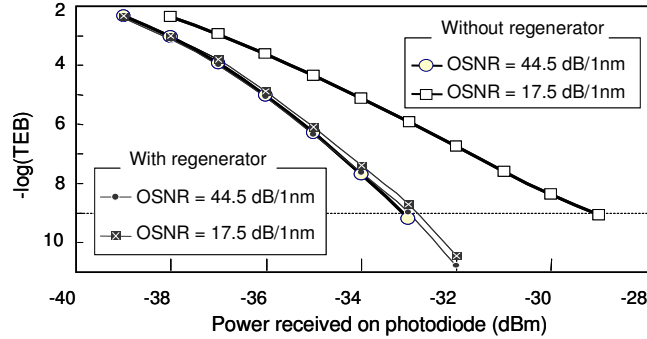


Fig. 8. BER evolution as a function of the power received on the photodiode.

Figure 9a shows the evolution of the BER as a function of the decision threshold. This curve provides a direct insight of the noise statistics. The slope of the flank is directly representative of intensity fluctuations: the steeper the flank is, the lower the noise amplitude is. The reference is in empty symbols and results with regenerator are in full symbols. In the presence of the regenerator, we observe that the flanks are steeper both on zero and one levels. This observation implies an improvement of the eye diagram opening. A useful parameter to evaluate the quality of the eye diagram is generally the Q-factor. But, after a regenerator the noise distributions are not Gaussian anymore and the Q-factor cannot be related to the minimum value of the BER as it is usually done [25]. However, using the data of Fig. 9a in the range  $10^{-9} < \text{BER} < 10^{-3}$ , we propose to calculate an equivalent Q-factor, obtained with the classical formula given in Ref [25]. This new parameter, called the eye-opening factor or E-factor, differs from the usual Q-factor in the sense that it cannot be used to deduce the minimum BER (except when noise distributions are Gaussian). The E-factor must be seen as a parameter allowing the measurement of the eye diagram quality when noise distributions are not Gaussian.

The ratio between the E-factor with and without the regenerator is the E-factor improvement. Figure 9b represents such a data for different values of the OSNR. A maximum value of E-factor improvement of 2.3 dB is obtained with an OSNR of 17.5 dB/1nm. For others values of the OSNR, the E-factor improvement is more than 1.6 dB. This implies that our regenerator improves the eye opening significantly over wide range of noise level.

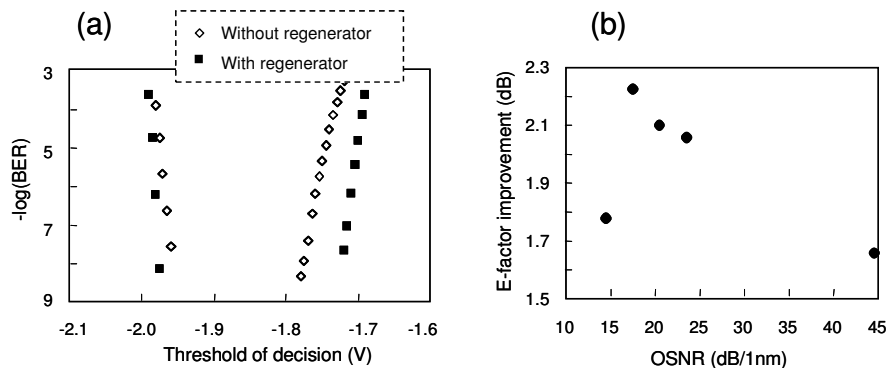


Fig. 9. (a) BER evolution as a function of the decision threshold for an OSNR of 17.5 dB/1nm; (b) Eye-opening improvement as a function of the OSNR.

### 3.3 Short recirculation loop measurements

The previous back-to-back measurements have allowed us to characterize the behavior of the regenerator in front of a receiver and have revealed some interesting features. Meanwhile,

these results are not sufficient to conclude neither on the ability of our device to improve the BER in a transmission link nor on the possibility to cascade the device. A very efficient way to answer this point is to test the regenerator in a short recirculation loop [26]. This tool is very similar to the usual recirculation loop except that the length of transmission fiber in the loop is restricted to several kilometers instead of hundreds of kilometers. This setup enables us to test the cascability and the ability of the regenerator to reduce the amplitude noise independently from the propagation effects. Figure 10 represents the setup of our short recirculation loop. We use a 10 km span of DSF fiber with a cumulated dispersion of  $-6$  ps/nm followed by an adequate dispersion compensating module. A noise source is coupled within the loop in order to assess the noise resistance of our regenerator. An EDFA and a variable attenuator are used together to keep the signal power in each loop at a constant value. The launched signal power into the 10 km span of DSF is 5 dBm. It is low enough to prevent any penalties due to nonlinear effects. A polarization controller is also used in the loop in order to minimize all the polarization issues.

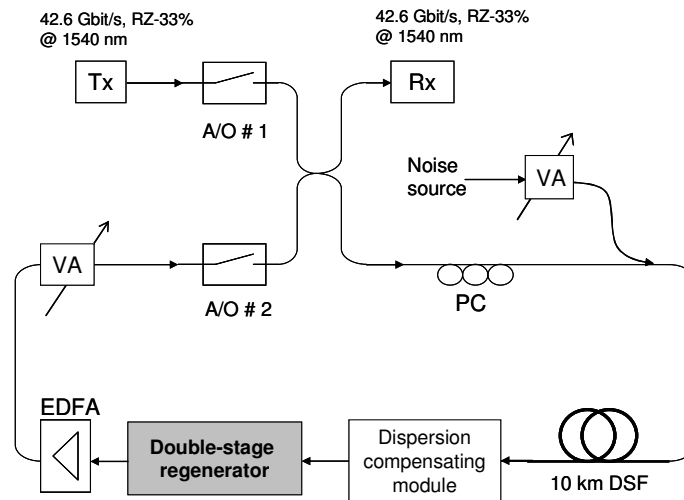


Fig. 10. Experimental setup of the short recirculation loop. Tx: Transmitter; Rx: Receiver; A/O: Accouter optical switch; PC: polarazation controller; VA: variable attenuator; DSF: dispersion shifted fiber; EDFA: Erbium doped fiber amplifier.

Figure 11a shows the evolution of the BER as a function of the number of laps in the loop with an OSNR of 23.5 dB/1nm. In the presence of the regenerator, the number of round trips is significantly improved. For example, for a BER of  $10^{-8}$ , 8 laps are performed without the regenerator whereas 24 laps are performed with the regenerator. This proves the efficiency and the cascability of our device. A critical parameter to evaluate the performance of a 2R is the noise resistance assessment (NRA), which corresponds to the ratio of the number of round trip reachable with ( $N_w$ ) and without ( $N_{wo}$ ) regeneration for a given BER and with the same OSNR at the first lap:  $NRA = N_w/N_{wo}$ . We measured the NRA for different values of OSNR. The results are plotted for a BER of  $10^{-8}$  and  $10^{-4}$  in Fig. 11b. We observe that the maximum NRA is equal to 4 for a BER =  $10^{-8}$  and to 10 for a BER =  $10^{-4}$ ; the minimum NRA is equal to 2 for a BER =  $10^{-8}$  and to 8 for a BER =  $10^{-4}$ .

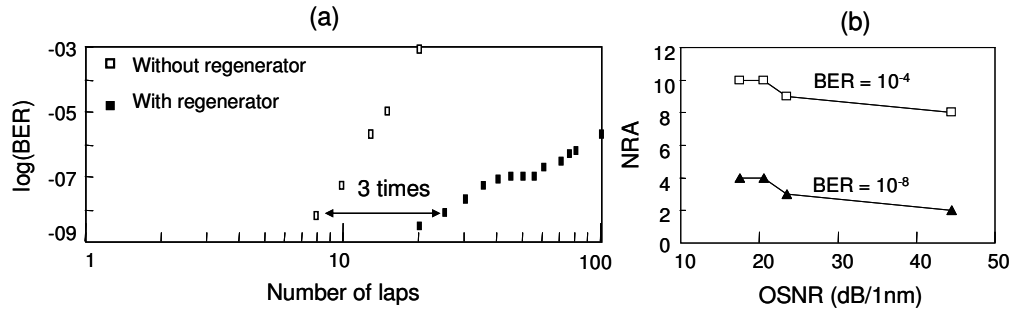


Fig. 11. (a) Evolution of BER as a function of laps in the loop, OSNR = 23.5 dB/1nm, 1 lap = 10 km; (b) Noise resistance assessment as a function of the OSNR for different output BER.

## 7. Conclusion

In this work, we have numerically and experimentally demonstrated the efficiency of a novel scheme for an all-optical 2R regenerator for RZ-33% 42.6 Gbit/s telecommunication systems. This new double stage device consists in a self-phase modulation based pulse compressor associated with a self-phase modulation based Mamyshev regenerator. The first compression stage is inserted in order to suppress the intrachannel nonlinear interactions due to pulse-to-pulse overlapping occurring in the second stage as well as to avoid any stimulated Brillouin backscattering phenomenon. The first compression stage is also spectrally shifted by means of an offset filtering so as to compensate for the frequency detuning occurring in the Mamyshev regenerator, thus remaining globally transparent to the signal wavelength.

A receiver sensitivity improvement of more than 5 dB was measured in a back-to-back configuration thanks to our regenerator, while an E-factor improvement of 2.3 dB was obtained. An experimental study of the cascability of the regenerator in a short recirculating loop setup has also shown an increase of a factor 10 in the achievable number of laps for a BER of  $10^{-4}$  with an OSNR of 17.5 dB/1nm. We finally believe that this kind of regenerator, especially designed for 42.6 Gbit/s RZ-33% optical telecommunication systems could find a large interest to improve the transmission system performances.